American Mineralogist, Volume 76, pages 1279–1290, 1991

Ascent of felsic magmas and formation of rapakivi

HANNA NEKVASIL
Department of Earth and Space Sciences, State University of New York, Stony Brook, New York 11794-2100, U.S.A.

ABSTRACT

The wide compositional range of rapakivi-bearing rocks strongly suggests that process, not composition, governs the formation of rapakivi texture. A computational investigation was undertaken to determine whether decompression can induce the formation of the common features of rapakivi, i.e., the presence of mantled ovoid megacrysts of alkali feldspar (occasionally with inclusions of plagioclase and quartz), embayed early-formed quartz, and the presence of two generations of the phenocrystic phases. Crystallization path calculations were conducted for seven rapakivi-bearing magma compositions at pressures in the range of 1–8 kbar to determine the effect of decompression on the phase stabilities of plagioclase, quartz, and alkali feldspar. These calculations indicate that decompression can produce parageneses that can lead to all of the characteristic features of rapakivi if (1) H_2O saturation is not attained prior to or during ascent, (2) the cooling rate during ascent lies in the range of ~5–10 °C/kbar, (3) ascent occurs after the magma has become saturated with both alkali feldspar and plagioclase, and (4) the temperature at the onset of decompression is low enough to prevent complete resorption of alkali feldspar during ascent. These constraints readily explain why rapakivi-bearing rocks are relatively uncommon in nature, although the compositions that could produce rapakivi are common and decompression is not an unusual process in the evolution of many felsic magmas.

INTRODUCTION

Many felsic igneous rocks are compositionally similar. The similarities in their bulk compositions and crystalline assemblages make it difficult to identify specific differences in their genetic histories. Therefore, any distinctive characteristics among felsic rocks (in their ferromagnesian minerals, in feldspar zoning, in their trace elements, etc.) become potential sources of important information. One distinctive characteristic is the presence of alkali feldspar mantled by plagioclase (rapakivi), which may provide a clue to the evolution of certain felsic rocks. Efforts to interpret the origin of rapakivi texture have been ongoing since the early work of Sederholm (1891) on the Fennoscandian rapakivi granites, yet no consensus regarding rapakivi-forming processes has emerged. Nonetheless, such efforts have yielded much petrographic (and more limited analytical and experimental) information on the characteristics of rapakivi that must be considered in evaluating any proposed model of their genesis.

Felsic extrusive and intrusive rocks containing rapakivi occur worldwide in spatial and temporal association with rocks as diverse as anorthosites (e.g., Scandinavia; Kranck, 1969), diorites (e.g., New Hampshire; Greenwood, 1951), and silicic rhyodacites (e.g., northern Arizona; Bladh, 1980). The general characteristics of rapakivi granites (and rhyolites) that have emerged from numerous studies of many such occurrences are the presence of rounded or "ovoid" megacrysts of perthitic microcline or orthoclase (rarely sanidine), showing incompletely resorbed boundaries that may or may not be rimmed by oligoclase (wiborgite-type or porphyritic-type, respectively, using the terminology of Wahl, 1925). (In this article, the term "rapakivi" will refer to both types.) Rapakivi-bearing rocks usually contain two generations of quartz and alkali feldspar (Tuttle and Bowen, 1958). Plagioclase is commonly found as phenocrysts and occasionally as crystals poikilitically included in alkali feldspar megacrysts (e.g., O'Leary Peak Porphyry, Arizona; Bladh, 1980). Early phenocrystic quartz often shows embayment of euhedral forms (e.g., Gold Butte, Montana; Volborth, 1962). Quartz is also found in the cores of megacrystic alkali feldspar (e.g., Gold Butte, Nevada; Volborth, 1962) and occasionally within plagioclase mantles (e.g., Red Beach Granite, Maine; Abbott, 1978). Although biotite (with hornblende) is the most commonly reported hydrous mineral, muscovite (Maine; Larabee et al., 1965) and riebeckite (e.g., New Hampshire; Greenwood, 1951) have also been found. In some cases, hydrous ferromagnesian minerals are absent and pyroxene is present (e.g., Adirondacks, New York; Buddington and Leonard, 1962). Miarolitic cavities indicating late stage volatile saturation have been commonly reported in rapakivi granites.

Analysis of feldspar and bulk rock compositions have been undertaken by numerous workers and indicate several general chemical trends. The Na_2O/K_2O ratios of bulk

0003–004X/91/0708–1279$02.00

rocks show wide variation (e.g., 0.42, Enchanted Rock Batholith, Texas; Hutchinson, 1956; 1.31, O'Leary Peak, Arizona; Bladh, 1980). However, based on a compilation of compositions of 37 rapakivi granites, Tuttle and Bowen (1958) concluded that rapakivi granites, in general, have a slightly higher orthoclase content than an average granite. Core compositions of alkali feldspar megacrysts are variable, reflecting the variability of the bulk rock Na_2O/K_2O ratios (Anderson, 1980), but most commonly range between Or_{68} and Or_{80} (Bladh, 1980) with low An contents. The plagioclase is usually oligoclase (An_{10}–An_{35}) (Bladh, 1980; Anderson, 1980). Although there is only slight variation between the compositions of mantle and phenocryst plagioclase, there is a tendency toward a slightly higher An content in the phenocrysts (Volborth, 1962; Ehrreich and Winchell, 1969).

Any process proposed for the formation of rapakivi texture must account for all of the above characteristic features. The compositional diversity (e.g., peraluminous to peralkaline and considerable variation in Na_2O/K_2O ratios) and variability in H_2O content found among rapakivi-bearing felsic rocks (as indicated by the presence of pyroxene in some and biotite in others) requires a relatively composition-independent process. Such a process must be very different from the one producing incompletely resorbed plagioclase rimmed by sodic alkali feldspar ("anti-rapakivi" texture) that occurs in rocks within a very specific compositional range (including H_2O content) (Nekvasil, 1990).

Since the early work of Sederholm (1891), many of the theories of rapakivi-forming processes that have been proposed are denied by the current state of our understanding of phase equilibria of felsic magmas. Tuttle and Bowen (1958), for example, attempted to use phase equilibria in the H_2O-saturated haplogranite system to postulate a rapakivi-forming process. They suggested that for a magma to produce rapakivi, the magma must crystallize alkali feldspar early, followed by quartz. Further crystallization would cause the H_2O content of the melt to increase to the point that the temperature would be low enough to result in intersection of the alkali feldspar solvus. At this point, plagioclase would join alkali feldspar and quartz, resulting in zonation of the feldspar from alkali feldspar to plagioclase. Coprecipitation of all three minerals would continue until failure of the overlying rock caused rapid decompression and the formation of a second generation of quartz and alkali feldspar. It is generally acknowledged, however, that H_2O contents of magmas will not increase much beyond the equilibrium saturation value for any given total pressure, although the kinetics of bubble formation might permit slight supersaturation. Therefore, it is not possible to increase the H_2O content of an H_2O-saturated melt by 100% (or more) by crystallization, as Tuttle and Bowen (1958) suggested. If, instead, crystallization occurred under H_2O-undersaturated conditions at a pressure high enough to result in a ternary eutectic in the haplogranite system upon attainment of H_2O saturation during unbuffered crystallization, then plagioclase could eventually be stabilized. However, as will be discussed below, ascent of H_2O-saturated magma will not result in the formation of rapakivi texture.

More recent models also recognize the important role that decompression might play in the formation of rapakivi-bearing rocks. Whitney (1975) briefly suggested that decompression of certain H_2O-undersaturated felsic magmas could result in crystallization of plagioclase from a magma that was crystallizing only alkali feldspar. This could be accompanied by partial (incomplete) resorption of the alkali feldspar. Cherry and Trembath (1978) expanded upon this idea by suggesting that decompression could produce rapakivi textures but, under either H_2O-undersaturated or H_2O-saturated conditions, by shifting a melt from equilibrium with plagioclase, quartz, and alkali feldspar to just plagioclase and quartz. However, the process requires disequilibrium crystallization at high pressure, large undercoolings during ascent, and rapid crystallization in a pressure quench process. As will be seen below, however, such a pressure quench process can only occur if H_2O-saturated conditions have been attained by the time of emplacement, and it will not lead to the characteristic features of rapakivi.

To date, none of the proposed rapakivi-forming processes has been adequately supported by either experimental or computational evidence. Although the role of decompression is now generally considered an important one, no constraints have been placed on this process with respect to the sequence of appearance of minerals, H_2O contents, requisite magnitude of the decompression events, bulk compositions of magmas, or the effects of decompression on the compositions of all phases involved. The experimental effort that would have to be expended to evaluate the effects of these variables is prohibitive. Therefore, a predictive computational model was used in the following analysis. This analysis evaluates the differences between the equilibrium state of each magma before and after decompression. These changes of state provide the driving potential for the time-dependent microscopic processes involved in the actual formation of the rapakivi textures. Discussion of these time-dependent processes themselves, however, is beyond the scope of this paper.

The revised quasi-crystalline model of Burnham and Nekvasil (1986) and Nekvasil (1986), the ternary feldspar solution model of Lindsley and Nekvasil (1989), and the crystallization path calculation methodology of Nekvasil (1988a) were used to investigate the possibility that decompression could drive a system to produce the characteristics of rapakivi. Extensive testing of the model (Nekvasil and Burnham, 1987; Nekvasil, 1988a) indicates that it can reliably predict phase relations in the system Ab-An-Or-Qz-H_2O. Most rapakivi-bearing rocks contain 85–99% of these components; therefore, the phase relations calculated for simple analogues should provide useful information regarding the natural systems.

Detailed equilibrium crystallization paths were calculated for seven rapakivi-bearing granites [Enchanted Rock

Batholith (ERB), Texas, Hutchinson, 1956; O'Leary Peak Pluton (OLP), Arizona, Bladh, 1980; Wolf River Batholith (WA-WRB), Wisconsin, Anderson and Cullers, 1978; Gold Butte (GB), Nevada, Volborth, 1962; Butler Hill (BH) granite, Missouri, Bickford et al., 1981; Deer Island (DI) and Crotch Island (CI), Maine, Stewart, 1959] in the pressure range of 1–8 kbar and several H_2O contents. The variations in proportions and compositions of all phases at these pressures, when compared with petrographic and chemical analysis of natural rapakivi-bearing rocks, permit the evaluation of the role of decompression in the formation of rapakivi texture.

PHASE RELATIONS OF RAPAKIVI-BEARING MAGMAS

Equilibrium crystallization paths for seven rapakivi-bearing rocks from the localities listed above were calculated at several pressures and H_2O contents. These paths assume that the bulk composition of each rock is similar to the magma from which it crystallized. The validity of this assumption is difficult to assess; however, if these bulk compositions can produce all the characteristics of rapakivi by the same process, the process will have been shown generally to be viable (although not necessarily specific to a given rock). If the rocks represent fractionates from a batholithic suite, then the unit investigated could represent a liquid. If some of the crystalline material present in a unit represents restite, then, as long as it was in equilibrium with a melt, the calculated equilibrium crystallization path of the bulk composition is still valid. If the rocks represent cumulates, then it should be very difficult to correlate the calculated crystallization paths (which are based on the bulk compositions) with the petrography. As will be shown below, this was not a problem for any of the compositions analyzed. The assumption is of most concern if there is evidence for assimilation of xenoliths after the megacrystic (early-formed) phases had crystallized. The compositions used in this study were selected to minimize the chances of late contamination playing a role (although this may have occurred in OLP; Bladh, 1980).

The bulk compositions for the seven samples were recast into normative Ab, Or, An, Qz for the modeling. Among the samples, these components summed between 86 and 99 wt%, with the majority lying near 95%. As seen in Table 1 (second column), the samples indicate a significant compositional range with renormalized normative Ab ranging from 28 to 44 wt%, Or from 24 to 39 wt%, Qz from 22 to 33 wt%, and An from 6 to 11 wt%. Such compositional variability should result in considerable differences in saturation temperatures of the three crystalline phases considered, their sequence of appearance, and even their compositions.

Sequence of appearance of crystalline phases

Table 1 shows the results of calculations conducted for the seven compositions at 2 and 5 kbar and 2.8 wt% (30 mol%) bulk H_2O (in the system). This H_2O content (between 2 and 3 wt%) was chosen as a demonstration because it lies approximately midway between the dry and H_2O-saturated values at low pressure and is that expected for equilibrium with biotite or amphibole (Burnham, 1979). The temperature of appearance of the liquidus mineral, the saturation temperatures of the second and third crystalline phases, and the H_2O-saturated solidus temperature are given for each composition. Additionally, the compositions and proportions of crystalline phases are given in order to indicate the effects of diversity in bulk compositions on the phase relations.

As anticipated, the compositional variability among the rocks selected for modeling results in considerable differences in saturation temperatures and sequence of appearance of the minerals plagioclase, quartz, and alkali feldspar at both 2 and 5 kbar. An important invariant characteristic, however, does emerge for all these compositions. Alkali feldspar is not the liquidus phase for any of these compositions at any pressure (between 1 and 8 kbar) or H_2O content (from dry to H_2O saturated). Several additional compositions (showing rapakivi texture, but not indicated in Table 1) were also investigated and yielded the same result. Plagioclase is the liquidus phase for all compositions in Table 1 at both 2 and 5 kbar. Additional investigation of another BHG composition (no. 177 in Bickford et al., 1981) shows quartz and plagioclase on the liquidus at 2 kbar and quartz on the liquidus at 5 kbar, indicating that plagioclase need not be the liquidus mineral. In fact, just as plagioclase or quartz could be the liquidus mineral for certain bulk compositions, there is no reason that alkali feldspar could not be the liquidus mineral for compositions with sufficiently low bulk An contents. Additionally, differences in pressure for a given bulk composition can change the identity of the liquidus phase for rocks in which the temperature of saturation of quartz and a feldspar are in close proximity.

The differences in bulk compositions among those studied also result in differences in the sequences of appearance of the nonliquidus phases, quartz and alkali feldspar (see Table 1). The sequence of appearance of these two minerals is a function of not only the bulk composition but also of the pressure and H_2O content. As indicated by the experiments of Whitney (1975) and the calculations of Nekvasil and Burnham (1987), the effect of isobarically increasing H_2O content is to increase the thermal stability of alkali feldspar relative to quartz, and the effect of increasing pressure at constant H_2O content is to decrease the stability of feldspar. Changes in these variables can induce a change in the sequence of appearance of quartz and alkali feldspar (see ERB in Table 1). As inferred from additional calculations using the compositions of Table 1, bulk H_2O contents of 0–3 wt% will generally result in quartz appearing before alkali feldspar; however, for higher bulk H_2O contents, alkali feldspar will commonly be the second crystalline phase to appear.

Several workers have previously suggested that alkali feldspar is not necessarily the liquidus mineral in rapakivi granites. Based on phase equilibrium constraints,

TABLE 1. Calculated phase relations at 2 and 5 kbar for seven rapakivi-bearing rocks with 2.8 wt% H_2O

Sample	Bulk composition Ab, Or, An, Qz (wt%)	Pressure (kbar)	Liquidus temperature (°C)	Liquidus phase composition (wt%)	Second mineral saturation *T* (°C)	Phase compositions (wt%)
ERB	$Ab_{34}Or_{30}An_{11}Qz_{25}$	5	1062	$An_{84}Ab_{15}Or_1$	882	Qz_{100} $An_{62}Ab_{36}Or_2$
		2	1038	$An_{82}Ab_{17}Or_1$	809	$Or_{73}Ab_{24}An_3$ $An_{45}Ab_{50}Or_5$
OLP	$Ab_{44}Or_{24}An_6Qz_{26}$	5	1001	$An_{70}Ab_{29}Or_1$	887	Qz_{100} $An_{44}Ab_{53}Or_3$
		2	978	$An_{66}Ab_{33}Or_1$	803	Qz_{100} $An_{25}Ab_{68}Or_7$
WA-WRB	$Ab_{31}Or_{39}An_8Qz_{22}$	5	1038	$An_{83}Ab_{16}Or_1$	890	$Or_{78}Ab_{18}An_4$ $An_{62}Ab_{35}Or_3$
		2	1012	$An_{82}Ab_{17}Or_1$	873	$Or_{76}Ab_{20}An_4$ $An_{59}Ab_{37}Or_4$
GB	$Ab_{82}Or_{34}An_{10}Qz_{28}$	5	1050	$An_{88}Ab_{11}Or_1$	905	Qz_{100} $An_{76}Ab_{23}Or_1$
		2	1026	$An_{86}Ab_{13}Or_1$	817	Qz_{100} $An_{58}Ab_{39}Or_3$
BHG	$Ab_{35}Or_{26}An_6Qz_{33}$	5	981	$An_{80}Ab_{19}Or_1$	944	Qz_{100} $An_{75}Ab_{24}Or_1$
		2	944	$An_{75}Ab_{24}Or_1$	844	Qz_{100} $An_{68}Ab_{30}Or_2$
DI	$Ab_{34}Or_{28}An_{11}Qz_{27}$	5	1069	$An_{86}Ab_{13}Or_1$	900	Qz_{100} $An_{68}Ab_{31}Or_1$
		2	1045	$An_{84}Ab_{16}Or_1$	813	Qz_{100} $An_{49}Ab_{48}Or_3$
CI	$Ab_{35}Or_{27}An_7Qz_{31}$	5	999	$An_{81}Ab_{18}Or_1$	930	Qz_{100} $An_{73}Ab_{26}Or_1$
		2	977	$An_{77}Ab_{22}Or_1$	841	Qz_{100} $An_{50}Ab_{48}Or_2$

Stewart (1959) concluded that, for DI and CI, precipitation of plagioclase and quartz preceeded precipitation of alkali feldspar. He indicated further that this conclusion was supported by the bulk compositions and petrography of the DI and CI rapakivi granites. Bladh (1980) concluded that plagioclase was the liquidus phase for the O'Leary Peak pluton, basing her conclusions on an experimental investigation of the OLP. The calculated results support these conclusions but indicate further that rapakivi-bearing magmas, in general, may rarely crystallize alkali feldspar as the liquidus mineral. Petrographic observations of inclusions of plagioclase ± quartz within many mantled alkali feldspar megacrysts lend support to the calculated results (e.g., plagioclase poikilitically included in microcline, ERB, Hutchinson, 1956; oligoclase inclusions in megacrystic sanidine, OLP, Bladh, 1980; inclusions of both plagioclase and quartz in alkali feldspar, WA-WRP, Anderson, 1980; quartz inclusions within mantled alkali feldspar, GB, Volborth, 1962).

The early phenocryst-forming stage of crystallization

To evaluate decompression as a mechanism for producing all the features of rapakivi, the assemblage before and after decompression must be considered. For rocks that contain two generations of crystalline phases, it is reasonable to presume that the early phenocrystic (or megacrystic) phases indicate the assemblage during the higher pressure stage of crystallization, and the matrix phases are those produced after emplacement, in the later stage of evolution. For all the compositions investigated (with the exception of ERB, which lacks early quartz), two generations of quartz, plagioclase, and alkali feldspar are reported, indicating an early assemblage containing all three crystalline phases. Comparison of the reported assemblages with those calculated in the pressure range 1–8 kbar can be used to obtain a reasonable pressure at which to model the formation of the early assemblages. In view of the wide compositional ranges of the feldspars

TABLE 1—*Continued*

Phase proportions (wt%)	Third mineral saturation T (°C)	Phase compositions (wt%)	Phase proportions (wt%)	Solidus temperature (°C)	Phase compositions (wt%)	Phase proportions (wt%)
0	842	$Or_{75}Ab_{22}An_3$	0	680	$Or_{77}Ab_{21}An_1$	37
12		Qz_{100}	4		Qz_{100}	25
		$An_{49}Ab_{47}Or_4$	18		$An_{26}Ab_{68}Or_5$	38
0	797	$Or_{73}Ab_{24}An_3$	2	724	$Or_{71}Ab_{27}An_2$	38
10		Qz_{100}	0		Qz_{100}	25
		$An_{44}Ab_{51}Or_5$	21		$An_{27}Ab_{66}An_7$	37
0	816	$Or_{62}Ab_{35}An_3$	0	675	$Or_{71}Ab_{28}An_1$	26
9		Qz_{100}	7		Qz_{100}	26
		$An_{23}Ab_{67}Or_{10}$	23		$An_{12}Ab_{78}Or_{10}$	48
0	775	$Or_{59}Ab_{38}An_3$	0	715	$Or_{63}Ab_{35}An_2$	27
19		Qz_{100}	3		Qz_{100}	26
		$An_{19}Ab_{70}Or_{11}$	27		$An_{12}Ab_{75}Or_{13}$	47
0	847	$Or_{78}Ab_{19}An_3$	10	680	$Or_{77}Ab_{22}An_1$	48
9		Qz_{100}	0		Qz_{100}	22
		$An_{56}Ab_{41}Or_3$	11		$An_{26}Ab_{68}Or_6$	30
0	771	$Or_{75}Ab_{22}An_3$	21	724	$Or_{72}Ab_{26}An_2$	52
10		Qz_{100}	0		Qz_{100}	22
		$An_{45}Ab_{41}Or_4$	15		$An_{28}Ab_{65}Or_7$	26
0	852	$Or_{79}Ab_{18}An_3$	0	682	$Or_{79}Ab_{20}An_1$	40
9		Qz_{100}	6		Qz_{100}	28
		$An_{62}Ab_{35}Or_3$	14		$An_{31}Ab_{64}Or_5$	32
0	817	$Or_{77}Ab_{20}An_3$	0	725	$Or_{74}Ab_{24}An_2$	43
14		Qz_{100}	5		Qz_{100}	28
		$An_{57}Ab_{40}Or_3$	15		$An_{33}Ab_{62}Or_5$	29
0	830	$Or_{71}Ab_{26}An_3$	0	675	$Or_{74}Ab_{25}An_1$	31
2		Qz_{100}	13		Qz_{100}	33
		$An_{38}Ab_{56}Or_6$	13		$An_{16}Ab_{76}Or_8$	36
0	793	$Or_{52}Ab_{46}An_2$	0	720	$Or_{68}Ab_{32}An_2$	34
5		Qz_{100}	8		Qz_{100}	33
		$An_{33}Ab_{60}Or_7$	15		$An_{17}Ab_{72}Or_{11}$	33
0	830	$Or_{75}Ab_{22}An_3$	0	679	$Or_{78}Ab_{21}An_1$	32
12		Qz_{100}	7		Qz_{100}	27
		$An_{49}Ab_{47}Or_4$	21		$An_{27}Ab_{67}Or_6$	41
0	792	$Or_{74}Ab_{23}An_3$	0	725	$Or_{72}Ab_{26}An_2$	35
20		Qz_{100}	2		Qz_{100}	27
		$An_{44}Ab_{51}Or_5$	23		$An_{28}Ab_{65}Or_7$	38
0	835	$Or_{72}Ab_{25}An_3$	0	676	$Or_{74}Ab_{25}An_1$	33
5		Qz_{100}	10		Qz_{100}	31
		$An_{41}Ab_{53}Or_6$	14		$An_{18}Ab_{74}Or_8$	36
0	798	$Or_{69}Ab_{28}An_3$	0	722	$Or_{68}Ab_{30}An_2$	36
10		Qz_{100}	5		Qz_{100}	31
		$An_{36}Ab_{58}Or_6$	16		$An_{18}Ab_{72}Or_{10}$	33

in these rocks and the limited effect of pressure on feldspar composition, such comparison does not provide a precise means of pressure determination. However, a distinct range does emerge from such comparisons.

For the OLP, Bladh (1980) reports an early phenocrystic stage consisting of plagioclase [$An_{26-11}Ab_{70-80}Or_{4-9}$ (mol%) phenocrysts and $An_{21-14}Ab_{72-78}Or_{7-10}$ inclusions in alkali feldspar], quartz, and alkali feldspar ($Or_{69-63}Ab_{30-36}$-An_1 megacrysts). The best agreement between these compositions and the calculated feldspar compositions (in the temperature range of multiple saturation with plagioclase and alkali feldspar) is found in the pressure range 4–5 kbar. For example, at 5 kbar, the calculated plagioclase and alkali feldspar compositions (from the onset of alkali feldspar crystallization to the solidus temperature) are $An_{22-11}Ab_{69-79}Or_{9-10}$ and $Or_{61-70}Ab_{36-29}An_{3-1}$ (in mol%, converted from Table 1), respectively. It may appear unusual that the calculated Or content of the alkali feldspar increases with decreasing temperature. It must be remembered that the H_2O content of the melt is continuously increasing and the lowered temperature results in a rotation of two-feldspar tie lines to more Or-rich alkali feldspar; additionally, the rapid decrease in Qz and Ab (through the precipitation of very Ab-rich plagioclase) will concentrate Or in the melt.

Similar comparisons of calculated and reported feldspar compositional ranges for compositions GB, BHG, and CI indicate that pressures between 4 and 6 kbar give the best agreement. ERB and DI, however, vary from this general trend. Hutchinson (1956) reports an early assemblage consisting of andesine (and oligoclase) and microcline without quartz for ERB. For this composition at 5 kbar and above, quartz is calculated to be the second crystalline phase to form for all H_2O contents other than that close to saturation. The absence of quartz, therefore, indicates a pressure of formation of the phenocrystic stage of significantly less than 5 kbar; the best agreement between the reported and calculated compositions is found

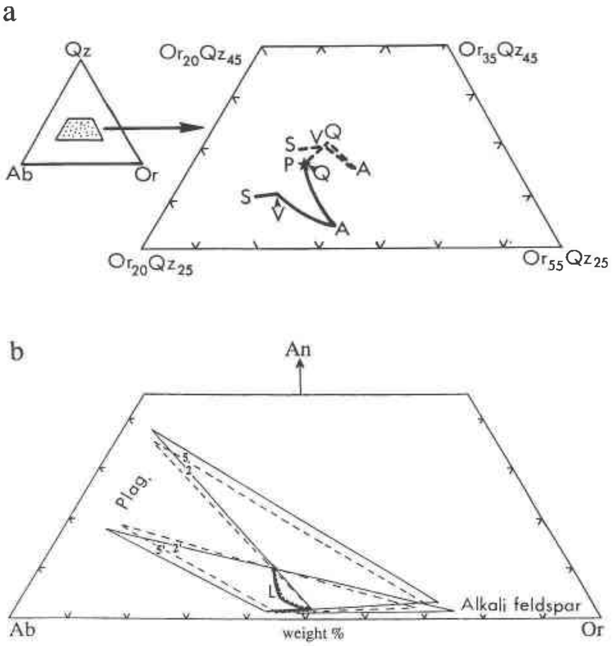

Fig. 1. Calculated equilibrium crystallization path at 2 kbar (dashed) and 5 kbar (solid) for a rapakivi granite from Crotch Island, Maine, with renormalized composition $Ab_{34.5}Or_{27.4}An_{6.9}Qz_{31.2}$ (wt%) given by the stars in **a** and **b** and bulk H_2O content of 2.8 wt%, projected (**a**) into the haplogranite system and (**b**) into the feldspar system. The crystallization paths are for H_2O-unbuffered conditions where the H_2O content in the melt increases during crystallization of anhydrous minerals. The symbols P (plagioclase), Q (quartz), A (alkali feldspar), and V (vapor) indicate the onset of appearance of each phase. S indicates the melt composition at the solidus temperature. The segment A-S indicates the variation of the melt when plagioclase, quartz, and alkali feldspar are coprecipitating (that is, as the melt moves across the four-phase surface in the granite system). The compositions of the feldspars at the onset of precipitation of the third phase and both feldspars at the solidus are shown for 5 kbar (triangles 5 and 5′) and 2 kbar (triangles 2 and 2′, respectively) in **b**.

at ~2 kbar. Inasmuch as this rock is similar in bulk composition to the other rocks (most notably, DI—see Table 1), the absence of quartz further indicates that the perturbation event that disrupted the formation of the early phenocrysts occurred at an earlier stage of the differentiation of the magma than for the other granites modeled. Although no analytical data are available on the exact compositions of the phenocrystic feldspars, this assertion is supported by the more calcic nature of andesine phenocrysts and mantles relative to the other granites (in which oligoclase is the most An-rich plagioclase). DI shows similar results, with the best agreement between the reported and calculated compositions at ~2 kbar, although in this case, the perturbation event occurred after the magma became multiply saturated with all three crystalline phases.

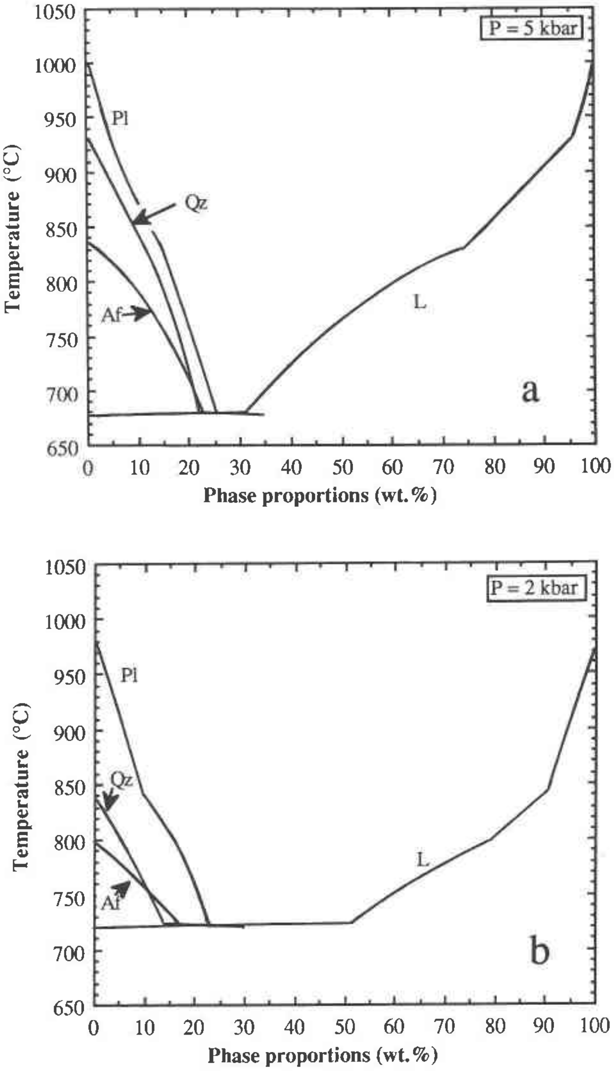

Fig. 2. Variations in the proportions of all phases during equilibrium crystallization are shown in (**a**) for 5 kbar and in (**b**) for 2 kbar for 2.8 wt% H_2O in the system for the paths in Figures 1a and 1b. The proportions of the crystalline phases (+ hydrous melt) have been renormalized to 100% after H_2O saturation is attained and vapor begins to exsolve. (Symbols: Pl, plagioclase; Af, alkali feldspar; Qz, quartz; L, hydrous melt.)

From these comparisons it appears that the pressure of formation of the early phases is not of major importance to the formation of rapakivi textures. However, since the phenocryst phase compositions for all bulk compositions except DI and ERB are consistent with an initial pressure of 5 kbar, this pressure was chosen as the pressure at which to model the formation of the early higher pressure phases. In order to determine the changes that would occur if the phenocrystic assemblages were perturbed by ascent of the magma, we must first be able to understand how the magma would have evolved isobarically. The CI composition is intermediate among the compositions chosen for study and will be used for demonstration purposes; the general trends discussed below, however, hold for all the compositions investigated.

Figures 1a and 1b show the evolution of the melt and crystals of a magma with composition CI, projected into the haplogranite system (Fig. 1a) and into the feldspar system (Fig. 1b) at 5 kbar (solid curve). The melt evolution path consists of four main segmental trends; the inflections indicate the appearance of a new phase. Moving from higher to lower temperature (i.e., from the bulk composition given by the star in Figs. 1a and 1b), the crystallization of plagioclase (beginning at P) results in depletion of An and Ab components and enrichment in Or and Qz. Once quartz appears (at Q), only Or will be significantly enriched in the melt. Finally, when alkali feldspar begins to precipitate (at A), the Qz content of the melt will increase until H_2O saturation is reached (at V) and the melt moved along the H_2O-saturated five-phase curve in the simple granite system (Nekvasil, 1988b) to the solidus composition (S). Figure 2a shows the variations in phase proportions during equilibrium crystallization at 5 kbar. The labeled inflections seen in Figures 1a and 1b correspond to the appearance of each new phase (including vapor at the lowest temperatures) in Figure 2a. The calculated compositions of the solid solutions at the onset of precipitation of each new phase and the solidus temperature are shown in Figure 1b and Table 1.

Figures 3a, 3b, and 3c show expanded views of the calculated variations in plagioclase, alkali feldspar, and quartz proportions, respectively, once all three crystalline phases have begun to coprecipitate. Alkali feldspar is the last phase to begin precipitating. Its abundance will, therefore, vary from zero to its solidus proportion. Some quartz and plagioclase are already present when alkali feldspar appears; their proportions, therefore, will not be zero at the highest temperature terminations of the phase proportion curves. The inflection in each curve of Figures 3a–3c marks the onset of vapor exsolution (H_2O saturation). Once the magma is H_2O saturated, cotecticlike crystallization occurs, resulting in large changes in phase proportions over a small temperature interval. These trends in variation of melt composition and phase proportions during isobaric crystallization are similar for all the compositions studied and generally characterize equilibrium crystallization paths of felsic magmas that are not H_2O buffered (Nekvasil, 1988b).

During isobaric crystallization along the four-phase curve in the granite system at 5 kbar, the phase proportions of plagioclase, quartz, and alkali feldspar all increase, albeit to different extents. For the composition CI

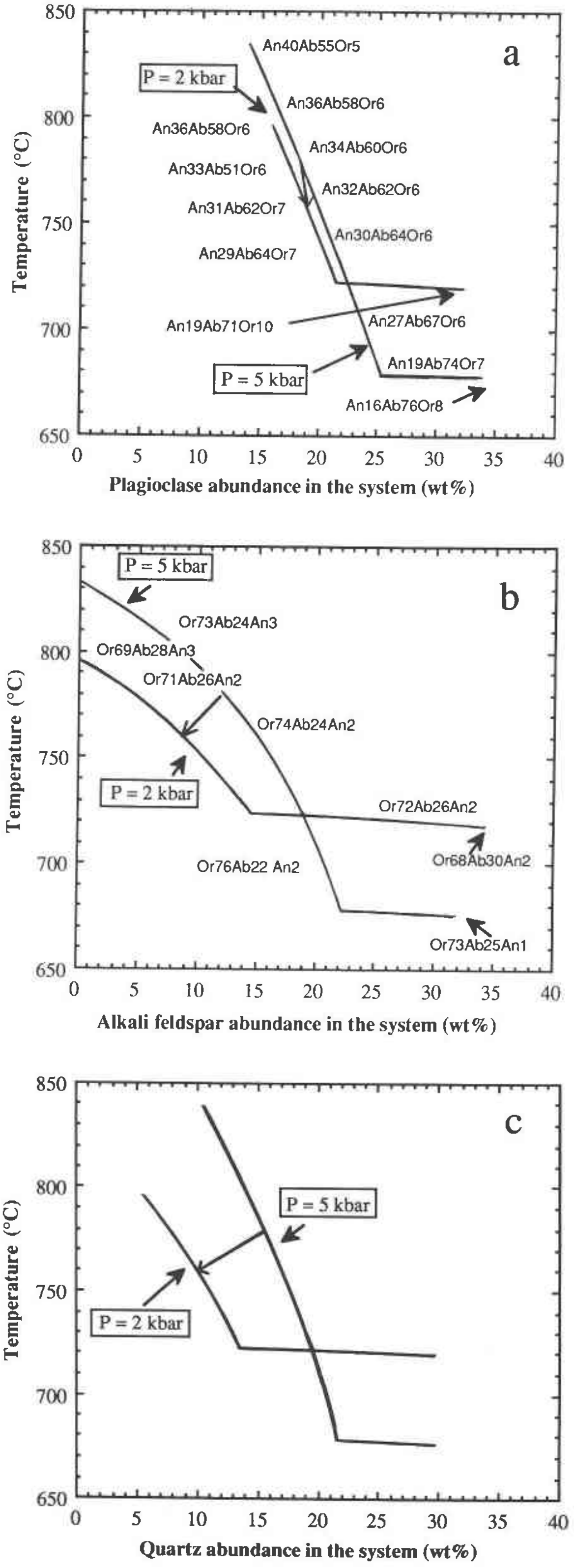

←

Fig. 3. Expanded view of the variation in phase proportions during equilibrium crystallization at 2 and 5 kbar for (**a**) plagioclase, (**b**) alkali feldspar, and (**c**) quartz. The variation in phase proportions in the system is shown only for crystallization across the four-phase surface (segments A-S in Fig. 1a) when the melt is multiply saturated with all three crystalline phases. Compositions indicated are given in weight percent. The arrow indicates the variation in phase proportions after decompression from 5 to 2 kbar starting at 780 °C with a 7 °C/kbar gradient.

at the onset of alkali feldspar saturation (at 5 kbar), the system consists of 74 wt% melt and 13% each of plagioclase and quartz (see Table 1). However, 50 °C below the alkali-feldspar saturation temperature, the proportion of alkali feldspar rises to 10 wt% of the system, whereas that of plagioclase rises to 18 wt% and of quartz to 15 wt%. The greater increase in proportion of alkali feldspar per degree of cooling (also shown by the shallow slope of the alkali feldspar curve in Fig. 3b) may result in the early formation of large crystals of alkali feldspar.

If ascent of a magma is required for the formation of rapakivi texture, then the viscosity must remain low enough during the early stages of crystallization to permit the magma to rise through the crust. The increase in crystallinity associated with cooling of a magma is the single most important factor in increasing the viscosity of the magma. It is, therefore, important that the magma become multiply saturated with the phenocrystic phases early in its differentiation history. Table 1 indicates the calculated variation in abundance of the crystalline phases as each magma cools from the liquidus to the solidus at 5 kbar. Importantly for all these compositions, multiple saturation with plagioclase, alkali feldspar, and quartz occurs when only 20–30 wt% of the system is crystalline.

The matrix-forming stage of crystallization

If the formation of a second generation of crystalline phases in rapakivi-bearing rocks is a result of perturbation caused by decompression, then the compositions of the matrix phases and the relative proportions of all phases (matrix and phenocrystic) should reflect low-pressure crystallization. However, unlike for the megacrystic phases, analytical data on the matrix feldspars are scarce, and this scarcity precluded use of the matrix compositions to estimate emplacement pressure. Therefore, for the analysis below, an emplacement pressure of 2 kbar is used as an example.

To identify differences between high- and low-pressure characteristics in the natural rocks, we must first look at variations in crystallization paths at different pressures. Figures 1a and 1b show the evolution of the CI bulk composition at 2 kbar juxtaposed against that at 5 kbar. Although the general trends are similar, a major difference in the Qz content of the evolving melts is apparent. As discussed in Nekvasil (1988b), the position of the H_2O-undersaturated four-phase surface in the granite system shifts to higher Qz contents with decreasing pressure. If the matrix phases represent melt after reequilibration at lower pressure, then the composition of the matrix should reflect a higher Qz content than that of the melt that was in equilibrium with the early formed phenocrystic phases.

In addition to the differences in the Qz content of melts crystallizing at 2 and 5 kbar in equilibrium with all three crystalline phases, there will also be slight differences in the An:Ab:Or ratios in the crystalline solid solutions at the two pressures. Figure 1b shows the calculated compositions of plagioclase and alkali feldspar when the melt reaches the four-phase surface (where an H_2O-undersaturated magma is in equilibrium with plagioclase, quartz, and alkali feldspar) at 5 and 2 kbar (triangles 5 and 2) and at the solidus temperatures (triangles 5′ and 2′), respectively. The differences in solidus feldspar compositions (i.e., higher Or content of the alkali feldspar but lower An content of the plagioclase at 5 kbar compared with those at 2 kbar) reflect the effect of pressure and temperature on the ternary feldspar solvus. Importantly, differences in the compositions of the solid solutions (plagioclase and alkali feldspar) are slight between the two pressures (as shown in Figs. 3a and 3b). These variations result in only slight differences in the solidus proportions of plagioclase and alkali feldspar (shown by the proportions at the terminations of the variation curves in Figs. 3a and 3b). (These small differences in the high- and low-pressure solidus phase proportions make it difficult to use bulk modal analyses to determine emplacement pressures because these variations in proportions lie within the uncertainty of most modal analyses.)

The calculated variations in phase proportions for CI at 2 kbar are shown in Figure 2b. The magnitude of the destabilizing effect of decreasing pressure on the crystalline phases varies considerably among the three crystalline phases. For quartz, lowering the pressure results in the greatest destabilization, which can be readily seen by comparing the quartz saturation temperatures at 5 and 2 kbar in Figure 2a (930 and 841 °C, respectively). For alkali feldspar, this destabilization results in a saturation temperature decrease from 835 °C at 5 kbar to 798 °C at 2 kbar. Plagioclase shows the least effect with only a 22 °C decrease in saturation temperature. Table 1 indicates the effect of decreasing pressure on the mineral saturation temperatures for all the compositions studied. For each crystalline phase, the extent of destabilization with decreasing pressure is generally independent of the bulk composition. For plagioclase, the extent of the destabilization is 8 ± 1 °C/kbar (higher for BHG), for alkali feldspar, 12 ± 1 °C/kbar (lower for WA-WRP), and for quartz, 29 ± 4 °C/kbar. It is these differences (in the extent of destabilization) among the crystalline phases that permit the formation of rapakivi textures by decompression.

DECOMPRESSION OF 2 FELDSPAR + QUARTZ + MELT (± VAPOR) ASSEMBLAGES

From petrographic evidence for all the samples, a perturbation event resulted in partial resorption of phenocrystic alkali feldspar (as evidenced by ovoid alkali feldspar in all the examples of Table 1), partial resorption of phenocrystic quartz (as evidenced by rounding and embayment in all but ERB), and continued precipitation of plagioclase (based on the absence of resorption textures, the persistence of euhedral forms on the phenocrysts, and the formation of mantles on the alkali feldspar). A second generation of each phase that crystallized earlier formed at the later stage.

For all compositions except ERB, the perturbation event (here modeled as decompression) must have occurred after the magma was multiply saturated with quartz, plagioclase, and alkali feldspar. The effects of decompression on these early formed phases in the rapakivi-bearing rocks were determined by investigating the changes induced in the phase proportions and compositions for several decompressional end points. These effects indicate the conditions under which decompression can produce rapakivi.

Thermal history

The simplest decompression thermal process of a magma, although unlikely to occur in nature, is isothermal decompression. If decompression from 5 to 2 kbar occurs isothermally, then the variations in phase compositions for CI can be obtained simply from Figures 3a–3c. If, for example, the system is at 780 °C at 5 kbar (with a phase assemblage of 12% alkali feldspar, 16% quartz, and 18% plagioclase) at the onset of decompression, the new assemblage at 2 kbar and 780 °C would consist of 5 wt% alkali feldspar, 8% quartz, and 17% plagioclase, if equilibrium were eventually reestablished at the lower pressure. [Although this temperature was chosen for ease of demonstration, it is interesting that feldspar geothermometry (of Fuhrman and Lindsley, 1988) at 5 kbar for the phenocrystic alkali feldspar and plagioclase pair $Or_{64}Ab_{34}An_2$ and $An_{18}Ab_{73}Or_9$, which lies within the range presented by Bladh, 1980 for the OLP, yields a temperature of 780 °C.] In this case, partial resorption of all three phases would take place, with plagioclase undergoing a small but definite amount of resorption. The decrease in phase abundances during decompression is nearly independent of the temperature at which ascent begins (as seen by the subparallel nature of the 2 and 5 kbar curves in Figs. 3a–3c) until the H_2O content at 5 kbar has reached the 2 kbar saturation value (5.7 wt% H_2O in the melt for CI). If this were the case, further crystallization at 5 kbar before ascent would result in quenching of the magma during ascent because of the lower H_2O solubility and hence higher solidus temperature at lower pressures (as can be seen in Figs. 3a–3c).

Ascent of natural magmas is most likely to take place with some finite loss of temperature. This can be adiabatic or nonadiabatic (and dependent upon the thermal regime, ascent rate, mode of ascent, and conductivity of the crust through which the magma is rising). The combination of low magmatic temperature at the onset of ascent and prior heating of the wall rocks could result in only a small average temperature loss during ascent, for example, 3–5 °C/kbar. As for isothermal decompression in this case, ascent must not commence before the temperature is low enough to retain all phases after decompression. However, because of the cooling during ascent, decompression could commence at a slightly higher temperature than for isothermal decompression without resulting in complete resorption of alkali feldspar. In Figures 3a–3c, for example, decompression could commence at or below 800 °C. If, for demonstration, we consider a temperature of 780 °C at the onset of decompression at 5 kbar and a temperature drop of 3 °C/kbar during ascent, then the phase assemblage changes from 12 wt% alkali feldspar, 16% quartz, and 18% plagioclase to 7% alkali feldspar, 9% quartz, and 18% plagioclase at 2 kbar. In contrast to isothermal decompression, the proportions of quartz and alkali feldspar decrease and that of plagioclase remains the same.

If the wall rocks were warm and ascent were sufficiently rapid, little heat would be lost from the magma during ascent and the temperature decrease of the magma would be close to adiabatic. Rumble (1976) and Sykes and Holloway (1987) calculated isentropic adiabats for hydrous albite melt in the presence of crystals (± vapor) and obtained gradients of ~ 7 °C/kbar. Using this value as an approximation for the multiphase, multicomponent adiabatic gradient, decompression from 5 to 2 kbar, beginning at 780 °C, would result in a lower pressure assemblage consisting of 9 wt% alkali feldspar, 10% quartz, and 19% plagioclase. This change in phase assemblage is consistent with what is observed in rapakivi-bearing rocks, that is, little perturbation of plagioclase, some resorption (rounding) of alkali feldspar, and more major embayment of quartz. As can be readily seen in Figures 3a–3c, average cooling rates greater than ~ 10 °C/kbar will result in precipitation of alkali feldspar instead of resorption.

From the examples above, it is readily noted that cooling rate during ascent plays a critical role in determining whether decompression will result in the characteristics of rapakivi. The maximum extent of resorption of alkali feldspar and quartz upon decompression occurs with only small amounts of cooling during ascent. However, very small amounts of cooling would also result in some resorption of plagioclase in addition to alkali feldspar and quartz. The precipitation of plagioclase can be maximized with larger cooling rates, but large cooling rates result in precipitation rather than resorption of alkali feldspar. The optimum cooling rate for the production of the characteristics of rapakivi is, therefore, only slightly higher than adiabatic, implying little heat loss to the wall rocks during ascent.

Although this discussion focuses on a closed system process, Figures 3a–3c can also illustrate the effects of an open system process such as a magma chamber recharge event. In this case, the temperature of the magma would increase isobarically, perhaps because of the influx of hotter, less differentiated magma. As can be readily seen in Figures 3a–3c, such an event would result in partial resorption of all crystalline phases, including plagioclase, and hence prohibit the formation of rapakivi texture.

The importance of H_2O content

The above discussion focused on the ascent of H_2O-undersaturated magma in which the magma remained H_2O undersaturated at the time of emplacement at the lower pressure. As was discussed for isothermal decompression, because of the lower H_2O solubilities at low pressure, it is possible that an H_2O-undersaturated magma could attain H_2O saturation during ascent. This becomes increasingly likely with large degrees of cooling during decompression. If the magma begins decompression at 740 °C and 5 kbar and cools at an average rate of 7 °C/kbar, the magma would be H_2O saturated once it reached 2 kbar (at 719 °C). In reflection of this, the phase assemblage would change from 17% alkali feldspar, 19% quartz, and 21% plagioclase to 25% alkali feldspar, 27% quartz, and 28% plagioclase (as can be seen in Figs. 3a–3c). No partial resorption of any crystalline phase would take place during ascent; instead, a considerable amount of crystallization (23%) would occur. Slightly larger decreases in temperature during decompression or a slightly lower temperature at the beginning of decompression would result in the magma cooling to the solidus temperature before 2 kbar were reached.

If H_2O saturation is attained prior to or during ascent or upon emplacement, a pressure quench phenomenon marked by rapid crystallization may take place that could result in a matrix-forming stage of evolution of the magma. However, as discussed above, this would not be accompanied by partial resorption of either quartz or alkali feldspar. Therefore, unlike Cherry and Trembath (1978), this author concludes that such a quench process would not produce rapakivi textures.

Magnitude of the decompression event

Decompression from 5 to 2 kbar has been discussed above. However, the main trends hold for any amount of decompression. Small changes in temperature are most conducive to the production of rapakivi textures, yet small changes in temperature also increase the likelihood of the loss of a phase during decompression, particularly for large changes in pressure. The lower the temperature at the onset of decompression, the less likely the loss of a phase becomes. However, the lower the initial temperature and, hence, the higher the degree of crystallinity, the more likely it becomes that the magma will become H_2O saturated before emplacement or that the viscosity becomes too high to permit much ascent. Thus, the conditions under which the formation of rapakivi is possible become increasingly restricted with larger pressure drops.

Compositional changes during ascent

One of the characteritics of rapakivi-bearing magmas is that, although texturally there is evidence of a major perturbation event, the compositions of the feldspars do not show marked discontinuities. In fact, for the compositions investigated, the large alkali feldspar ovoids are similar in composition to the matrix alkali feldspar, and plagioclase inclusions (within the alkali feldspar), early phenocrysts, and mantles are often indistinguishable in composition. Stewart (1959), for example, presents compositions of alkali feldspar in the groundmass for CI, which, when compared with his megacryst compositions, yield a maximum change in the feldspar compositions resulting from the perturbation event. He reports the presence of ovoid Or_{74} alkali feldspar megacrysts and Or_{69} alkali feldspar in the groundmass. (The outer zones of unmantled phenocrysts lie between Or_{72} and Or_{67}.) Bladh (1980) reports compositions of early plagioclase in OLP within the range $An_{21-14}Ab_{72-78}Or_{7-10}$, whereas clear plagioclase mantles on the alkali feldspar are of composition $An_{14}Ab_{76}Or_9$, also indicating very little change. Although subsolidus reequilibration of alkali feldspar may have occurred to smooth compositional differences, the sluggish kinetics of diffusion in plagioclase (Johannes, 1978) indicate that such reequilibration of plagioclase is unlikely.

The calculated results indicate that these small changes in feldspar compositions are fully consistent with decompression as the perturbation event. Figures 3a and 3b indicate the compositions of plagioclase and alkali feldspar at selected points along the phase assemblage curves for the CI bulk composition. Taking as an example a decompression event from 5 to 2 kbar starting at 780 °C with a temperature drop of 7 °C/kbar, the plagioclase composition changes from $An_{34}Ab_{60}Or_6$ to $An_{31}Ab_{62}Or_7$ (as shown in Figs. 3a and 3b). The calculated alkali feldspar composition changes from $Or_{73}Ab_{24}An_3$ to $Or_{71}Ab_{27}An_2$. These changes are very similar to those reported by Stewart (1959). All of the compositions investigated similarly show only small differences in the calculated (and reported) compositions of the phenocryst and matrix feldspars.

The effect of decompression from 5 to 2 kbar on the melt composition of CI can be readily seen in Figures 1a and 1b. As discussed above, the increase in silica content of the melt at lower pressures reflects the difference in position of the four-phase surface (plagioclase, quartz, alkali feldspar, and melt) at 5 kbar and 2 kbar. If the matrix of each of the rapakivi-bearing rocks represents the liquid after decompression, then its composition should lie on the low-pressure four-phase surface in the granite system. The increase in silica content of the melt that would be required to establish a new equilibrium could be achieved by partial resorption of phenocrystic quartz. Embayment of quartz is a common characteristic of rapakivi-bearing rocks and is reported for all of the compositions studied except ERB.

CONCLUSIONS

Investigation of the phase stabilities of several rapakivi-bearing magmas indicates that decompression can produce all of the features of rapakivi texture. This includes partial resorption of alkali feldspar and quartz, continued crystallization of plagioclase, small changes in alkali feldspar and plagioclase compositions, and the formation of two generations of the early formed phenocrystic phases. Many felsic magmas are considered to have crystallized at a higher level than that at which they were formed; yet, rapakivi-bearing rocks are rare enough to be noteworthy. Ascent alone, therefore, will not necessarily produce rapakivi. Instead several constraints on the decompression event must be met.

1. The bulk composition must be sufficiently Or rich to permit saturation with alkali feldspar and plagioclase during the early stages of differentiation. This ensures that

the H_2O content of the melt will not be very high at the onset of decompression. It also ensures that the degree of crystallinity will be low enough to permit ascent of the magma after saturation with alkali feldspar. Compositions classified as granites, granodiorites, and alkali granites (and their volcanic equivalents) readily fall into this category. Either diorites do not crystallize alkali feldspar, or they do so too late in their differentiation history to permit the formation of rapakivi. Syenites and trachytes form from higher temperature magmas and may go through a region of instability of plagioclase (Nekvasil, 1990), making the formation of rapakivi more difficult.

2. The H_2O content of the melt at the onset of decompression must be low enough that the magma will not become H_2O saturated during ascent. If the final pressure is 2 kbar, this requires melt H_2O contents at the onset of decompression of 5 wt% or less. (If emplacement occurs at even lower pressure, this H_2O content must be correspondingly less.) Although low H_2O content at the onset of decompression could be most readily assured if the bulk H_2O content of the system were low, an H_2O-rich magma might also produce rapakivi if the bulk composition permits saturation with plagioclase and alkali feldspar at a very early stage and decompression takes place soon thereafter.

3. The percentage of alkali feldspar that crystallizes at the higher pressure must be high enough so that ascent will not result in complete resorption of alkali feldspar. This constraint, along with the requirements for low H_2O content and crystallinity, places severe restrictions on temperature at the onset of ascent.

4. The change in temperature during decompression must be close to the adiabatic gradient. Large degrees of cooling ($\gtrsim 10$ °C/kbar) will result in precipitation, rather than partial resorption, of alkali feldspar during ascent. Very small degrees of cooling ($\lesssim 3$ °C/kbar) will result in partial resorption of plagioclase along with quartz and alkali feldspar and a greater possibility of complete resorption of alkali feldspar during decompression. This restriction could explain why rapakivi granites are so commonly found with nonrapakivi-bearing granites and other nonfelsic rocks. If the formation of rapakivi requires gradients close to adiabatic, then the country rock through which the magma ascends must have been prewarmed to prevent considerable heat loss during ascent.

This investigation has outlined the changes in equilibrium assemblages with decreasing pressure that could provide the driving force for the production of all of the textural characteristics of rapakivi. The results of this investigation indicate that a simple process such as decompression of a closed system and the reestablishment of equilibrium can produce parageneses that can lead to the formation of rapakivi. However, this does not imply that more complicated disequilibrium, open system processes such as magma mixing (e.g., Hibbard, 1981) cannot play a role. Therefore, the interpretation of the origin of rapakivi in a specific body must still be made on an individual basis after consideration of not only phase equilibria but also information about open system processes, provided for example, by textural and isotopic analysis.

ACKNOWLEDGMENTS

I thank J.R. Holloway, S.E. Swanson, J.A. Whitney, and D.H. Lindsley for critical reviews that significantly improved the manuscript and C.R. Bacon for editorial handling. This work was supported in part by NSF grant EAR-8916050 which is greatly appreciated. SUNY at Stony Brook provided generous computational support.

REFERENCES CITED

Abbott, R.N. (1978) Peritectic reactions in the system An-Ab-Or-Qz-H_2O. Canadian Mineralogist, 16, 245–256.

Anderson, J.L. (1980) Mineral equilibria and crystallization conditions in the late Precambrian Wolf River Massif, Wisconsin. American Journal of Science, 280, 289–332.

Anderson, J.L., and Cullers, R.L. (1978) Geochemistry and evolution of the Wolf River Batholith, a late PreCambrian rapakivi massif in northern Wisconsin, U.S.A. PreCambrian Research, 7, 287–324.

Bickford, M.E., Sides, J.R., and Cullers, R.L. (1981) Chemical evolution of magmas in the Proterozoic terrane of the St. Francois mountains, southeastern Missouri: 1. Field, petrographic and major element data. Journal of Geophysical Research, 86, 10365–10386.

Bladh, K.L. (1980) Rapakivi texture from the O'Leary Porphyry, Arizona. Bulletin Volcanologique, 43, 155–171.

Buddington, A.F., and Leonard, B.V. (1962) Regional geology of the St. Lawrence County magnetite district Northwest Adirondacks, NY. U.S. Geological Survey Professional Paper, 376, 1–259.

Burnham, C.W. (1979) The importance of voltatile constituents. In H.S. Yoder, Ed., The evolution of the igneous rocks, p. 439–482. Princeton University Press, Princeton, New Jersey.

Burnham, C.W., and Nekvasil, H. (1986) Equilibrium properties of granite pegmatite magmas. American Mineralogist, 71, 239–263.

Cherry, M.E., and Trembath, L.T. (1978) The pressure quench formation of rapakivi texture. Contributions to Mineralogy and Petrology, 68, 1–6.

Ehrreich, A.L., and Winchell, R.E. (1969) Rapakivi texture in rhyolite. Nature, 224, 905–906.

Fuhrman, M.L., and Lindsley, D.H. (1988) Ternary-feldspar modeling and thermometry. American Mineralogist, 73, 201–215.

Greenwood, R. (1951) Younger intrusive rocks of Plateau Province, Nigeria, compared with the alkaline rocks of New England. Geological Society of America Bulletin, 62, 1151–1178.

Hibbard, M.J. (1981) The magma mixing origin of mantled feldspars. Contributions to Mineralogy and Petrology, 76, 158–170.

Hutchinson, R.M. (1956) Structure and petrology of the Enchanted Rock batholith, Llano and Gillespie Counties, Texas. Geological Society of America Bulletin, 67, 763–806.

Johannes, W. (1978) The melting of plagioclase in the system Ab-An-H_2O and Qz-Ab-An-H_2O at P_{H_2O} = 5 kbar, an equilibrium problem. Contributions to Mineralogy and Petrology, 66, 295–303.

Kranck, E.H. (1969) Anorthosites and rapakivi magmas from the lower crust. New York State Museum and Science Service Memoir, 18, 93–97.

Larabee, D.M., Spencer, C.W., and Swift, D.J.P. (1965) Bedrock geology of the Grand Lake area Aroostook, Hancock, Penobscot and Wash counties, Maine. U.S. Geological Survey Bulletin, 1201-E, E1–E38.

Lindsley, D.H., and Nekvasil, H. (1989) A ternary model for all reasons. Eos, 70, 506.

Nekvasil, H. (1986) A theoretical thermodynamic investigation of the system Ab-An-Or-Qz(-H_2O) with implications for melt speciation. Ph.D. thesis, The Pennsylvania State University, University Park, Pennsylvania.

——— (1988a) The calculation of crystallization paths of compositionally simple felsic melts. American Mineralogist, 73, 956–965.

——— (1988b) Calculated effect of anorthite component on the crystallization paths of H_2O-undersaturated haplogranitic melts. American Mineralogist, 73, 966–982.

——— (1990) reaction relations in the granite system: Implications for trachytic and syenitic magmas. American Mineralogist, 75, 560–571.

Nekvasil, H., and Burnham, C.W. (1987) The calculated individual effects of pressure and H_2O content on phase equilibria in the granite system. The Geochemical Society Special Publication, 1, 433–446.

Rumble, D. (1976) The adiabatic gradient and adiabatic compressibility. Carnegie Institution of Washington Year Book, 75, 651–655.

Sederholm, J.J. (1891) Über die finnlandischen Rapakiwigesteine. Tschermaks Mineralogische und Petrologische Mitteilungen, 12, 1–30.

Stewart, D.B. (1959) Rapakivi granite from eastern Penobscot Bay, Maine. International Geological Congress Session 20, Sec. 11, 293–320.

Sykes, M.L., and Holloway, J.R. (1987) Evolution of granitic magma during ascent: A phase equilibrium model. The Geochemical Society Special Publication, 1, 447–461.

Tuttle, O.F., and Bowen, N.L. (1958) The origin of granite in light of experimental studies in the system $NaAlSi_3O_8$-$KAlSi_3O_8$-SiO_2-H_2O. Geological Society of America Memoir, 74, 153 p.

Volborth, A. (1962) Rapakivi-type granites in the Precambrian Complex of Gold Butte, Clark County, Nevada. Geological Society of America Bulletin, 73, 813–832.

Wahl, W. (1925) Die Gesteine des Wiborger Rapakiwigebietes. Fennia, 45, 105–126.

Whitney, J.A. (1975) The effect of pressure, temperature, and X_{H_2O} on phase assemblage in four synthetic rock compositions. Journal of Geology, 83, 1–31.

MANUSCRIPT RECEIVED FEBRUARY 13, 1990
MANUSCRIPT ACCEPTED APRIL 17, 1991